12

Pyramid Solid Elements

TABLE OF CONTENTS

§12.1. Introduction

Pyramid solid elements are useful for transition between bricks and tetrahedra in automated 3D mesh generation. Figure 12.1 depicts the 3 elements developed in this Chapter. Elements with 5, 13 and 14 nodes are identified as `Pyra5`, `Pyra13` and `Pyra14`, respectively, in the sequel. A brief description follows.
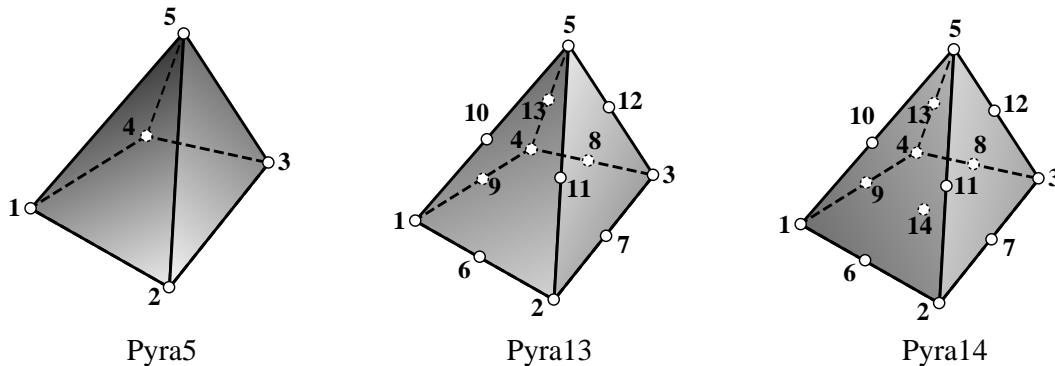

FIGURE 12.1. The three pyramid elements considered in this Chapter.

`Pyra5`. A isoparametric 5-node pyramid element that is useful as transition between 8-node bricks and 4-node tetrahedra. Although this element was available in several solid codes developed since 1972 (and presently in several general purpose FEM codes, notably ANSYS), the rederivation here serves to illustrate some aspects of the derivation and implementation of the more complicated elements.

`Pyra13`. A isoparametric 13-node pyramid element obtained from `Pyra5` by adding 8 midside nodes. It is useful as transition between 20-node (serendipity) bricks and 10-node tetrahedra.

`Pyra14`. A isoparametric 14-node pyramid element derived from `Pyra13` by injecting a node at the center of the quadrilateral face. It is useful as transition between 27-node (Lagrangian) bricks and 10-node tetrahedra.

The shape function set for `Pyra5` is unique and has been known since the early 1970s. The sets for `Pyra13` and `Pyra14` are not unique. Some instances were implemented in mid-1970 proprietary codes used by the nuclear reactor industry of the time. The shape functions presented here are instances of a parametric family obtainable through the template approach. It was felt that a comprehensive but lengthy derivation of all possible sets was not worthwhile because these elements fulfill a limited function.

§12.2. Geometric Description

The major ingredients of the pyramid geometry are illustrated in Figure 12.2. A pyramid has 5 corners, 8 edges and 5 faces. One of the faces is a quadrilateral, called the *base*, which may be warped. The corner opposite to the base is the *apex*. Four triangular faces, called *apex faces*, meet at the apex. The apex faces are planar in `Pyra5` but may be warped in `Pyra13` and `Pyra14`.
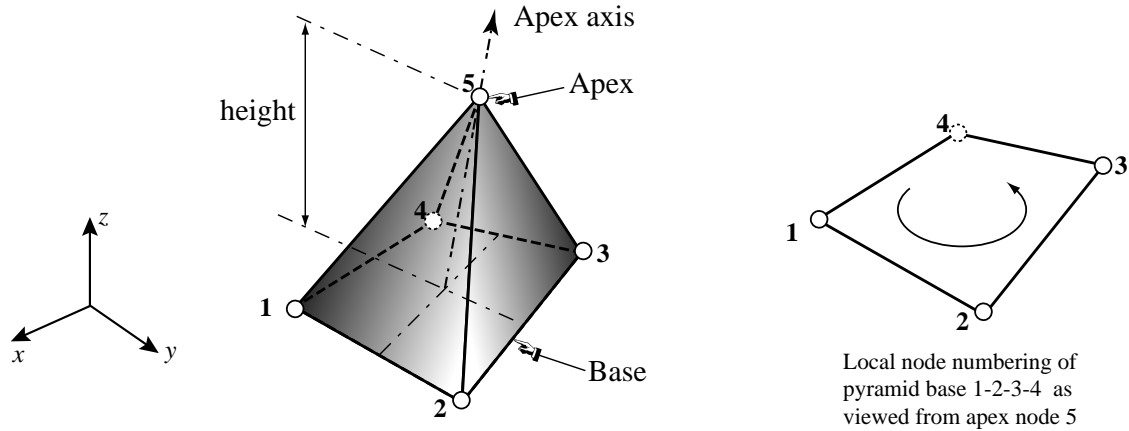
FIGURE 12.2. Nomenclature for pyramid geometry.

By analogy to pyramidal monuments, the normal distance from the quadrilateral base to the apex is called the *height*. The line joining the base center with the apex is the *apex axis*. This *apex direction* is not generally normal to the base.

§12.3. The Isoparametric Definition

This section summarizes the formulation of element stiffness and mass matrices of arbitrary isoparametric (iso-P) solid elements. The following formulation steps are well know; this material serves primarily to introduce notation.

An iso-P solid element has n nodes of global Cartesian coordinates $\{x_i, y_i, z_i\}$, $i = 1, 2, \ldots n$, which define the geometry of the element. The node displacements are $\{u_{xi}, u_{yi}, u_{zi}\}$, which are stacked node-wise to form the $3n \times 1$ node displacement vector $\mathbf{u}^{(e)}$.

The global coordinates of a generic point P in the element are $\{x, y, z\}$ and the displacement components at P are $\{u_x, u_y, u_z\}$ its displacement components.
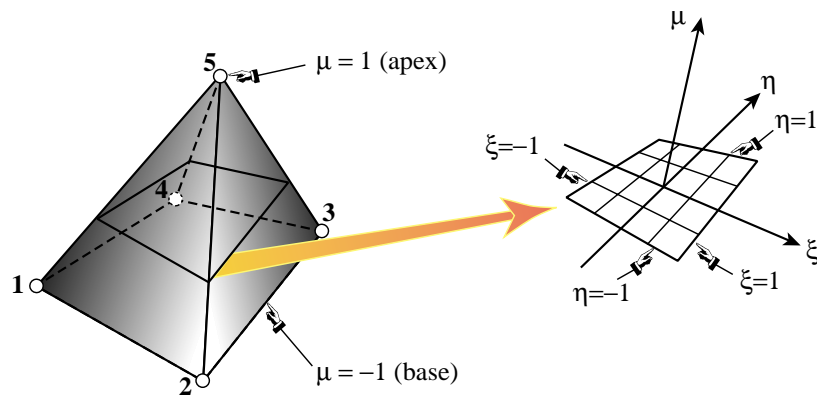

FIGURE 12.3. The natural coordinates (ξ, η, μ) for the pyramid element.

All elements considered here employ the natural coordinates $\{\xi, \eta, \mu\}$ of brick and brick-like elements, which range from -1 to $+1$. For the special case of the pyramid geometry those coordinates

are illustrated in Figure 12.3. Coordinate μ is special in that it identifies the apex direction.

The shape functions are denoted by $N_i = N_i(\xi, \eta, \mu)$. The isoparametric definition of a 3D element with n nodes is

$$
\begin{bmatrix} 1 \\ x \\ y \\ z \\ u_x \\ u_y \\ u_z \end{bmatrix} = \begin{bmatrix} 1 & 1 & 1 & 1 & \ldots & 1 \\ x_1 & x_2 & x_3 & x_4 & \ldots & x_n \\ y_1 & y_2 & y_3 & y_4 & \ldots & y_n \\ z_1 & z_2 & z_3 & z_4 & \ldots & z_n \\ u_{x1} & u_{x2} & u_{x3} & u_{x4} & \ldots & u_{xn} \\ u_{y1} & u_{y2} & u_{y3} & u_{y4} & \ldots & u_{yn} \\ u_{z1} & u_{z2} & u_{z3} & u_{z4} & \ldots & u_{zn} \end{bmatrix} \begin{bmatrix} N_1 \\ N_2 \\ N_3 \\ N_4 \\ \vdots \\ N_n \end{bmatrix}. \tag{12.1}
$$

For later use in the expression of the mass matrix, define

$$
\begin{bmatrix} u_x \\ u_y \\ u_z \end{bmatrix} = \begin{bmatrix} N_1 & 0 & 0 & N_2 & 0 & 0 & \ldots 0 \\ 0 & N_1 & 0 & 0 & N_2 & 0 & \ldots 0 \\ 0 & 0 & N_1 & 0 & 0 & N_2 & \ldots N_n \end{bmatrix} \begin{bmatrix} u_{x1} \\ u_{y1} \\ u_{z1} \\ \vdots \\ u_{zn} \end{bmatrix} = \mathbf{N}\mathbf{u}^{(e)}. \tag{12.2}
$$

The entries of the 3×3 Jacobian $\mathbf{J}$ of $\{x, y, z\}$ with respect to $\{\xi, \eta, \mu\}$ are given by

$$
\mathbf{J} = \frac{\partial(x, y, z)}{\partial(\xi, \eta, \mu)} = \begin{bmatrix} \partial x/\partial\xi & \partial y/\partial\xi & \partial z/\partial\xi \\ \partial x/\partial\eta & \partial y/\partial\eta & \partial z/\partial\eta \\ \partial x/\partial\mu & \partial y/\partial\mu & \partial z/\partial\mu \end{bmatrix} = \begin{bmatrix} J_{x\xi} & J_{y\xi} & J_{z\xi} \\ J_{x\eta} & J_{y\eta} & J_{z\eta} \\ J_{x\mu} & J_{y\mu} & J_{z\mu} \end{bmatrix},
$$

$$
J_{x\xi} = \sum_{i=1}^{n} \frac{\partial N_i}{\partial\xi} x_i, \quad J_{x\eta} = \sum_{i=1}^{n} \frac{\partial N_i}{\partial\eta} x_i, \quad J_{x\mu} = \sum_{i=1}^{n} \frac{\partial N_i}{\partial\mu} x_i,
$$

$$
J_{y\xi} = \sum_{i=1}^{n} \frac{\partial N_i}{\partial\xi} y_i, \quad J_{y\eta} = \sum_{i=1}^{n} \frac{\partial N_i}{\partial\eta} y_i, \quad J_{y\mu} = \sum_{i=1}^{n} \frac{\partial N_i}{\partial\mu} y_i, \tag{12.3}
$$

$$
J_{z\xi} = \sum_{i=1}^{n} \frac{\partial N_i}{\partial\xi} z_i, \quad J_{z\eta} = \sum_{i=1}^{n} \frac{\partial N_i}{\partial\eta} z_i, \quad J_{z\mu} = \sum_{i=1}^{n} \frac{\partial N_i}{\partial\mu} z_i,
$$

The inverse Jacobian is

$$
\mathbf{J}^{-1} = \frac{\partial(\xi, \eta, \mu)}{\partial(x, y, z)} = \begin{bmatrix} \partial\xi/\partial x & \partial\eta/\partial x & \partial\mu/\partial x \\ \partial\xi/\partial y & \partial\eta/\partial y & \partial\mu/\partial y \\ \partial\xi/\partial z & \partial\eta/\partial z & \partial\mu/\partial z \end{bmatrix} = \begin{bmatrix} J_{\xi x} & J_{\eta x} & J_{\mu x} \\ J_{\xi x} & J_{\eta y} & J_{\mu y} \\ J_{\xi z} & J_{\eta z} & J_{\mu z} \end{bmatrix}
$$

$$
= \frac{1}{J} \begin{bmatrix} J_{y\eta}J_{z\mu} - J_{y\mu}J_{z\eta} & J_{y\mu}J_{z\xi} - J_{y\xi}J_{z\mu} & J_{y\xi}J_{z\eta} - J_{y\eta}J_{z\xi} \\ J_{x\mu}J_{z\eta} - J_{x\eta}J_{z\mu} & J_{x\xi}J_{z\mu} - J_{x\mu}J_{z\xi} & J_{x\eta}J_{z\xi} - J_{x\xi}J_{z\eta} \\ J_{x\eta}J_{y\mu} - J_{x\mu}J_{y\eta} & J_{x\mu}J_{y\xi} - J_{x\xi}J_{y\mu} & J_{x\xi}J_{y\eta} - J_{x\eta}J_{y\xi} \end{bmatrix},
$$

where $\quad J = \det(\mathbf{J}) = J_{x\xi}J_{y\eta}J_{z\mu} + J_{x\eta}J_{y\mu}J_{z\xi} + J_{x\mu}J_{y\xi}J_{z\eta} - J_{x\mu}J_{y\eta}J_{z\xi} - J_{x\xi}J_{y\mu}J_{z\eta} - J_{x\eta}J_{y\xi}J_{z\mu}.$

$$\tag{12.4}$$

The Cartesian derivatives of the shape functions follow as

$$
\begin{aligned}
N_{xi} &= \frac{\partial N_i}{\partial x} = \frac{\partial N_i}{\partial \xi} J_{\xi x} + \frac{\partial N_i}{\partial \eta} J_{\eta x} + \frac{\partial N_i}{\partial \mu} J_{\mu x}, \\
N_{yi} &= \frac{\partial N_i}{\partial y} = \frac{\partial N_i}{\partial \xi} J_{\xi y} + \frac{\partial N_i}{\partial \eta} J_{\eta y} + \frac{\partial N_i}{\partial \mu} J_{\mu y}, \\
N_{zi} &= \frac{\partial N_i}{\partial z} = \frac{\partial N_i}{\partial \xi} J_{\xi z} + \frac{\partial N_i}{\partial \eta} J_{\eta z} + \frac{\partial N_i}{\partial \mu} J_{\mu z},
\end{aligned}
\tag{12.5}
$$

or in matrix form

$$
\begin{bmatrix} N_{xi} \\ N_{yi} \\ N_{zi} \end{bmatrix} = \begin{bmatrix} \partial N_i/\partial x \\ \partial N_i/\partial y \\ \partial N_i/\partial z \end{bmatrix} = \mathbf{J}^{-1} \begin{bmatrix} \partial N_i/\partial \xi \\ \partial N_i/\partial \eta \\ \partial N_i/\partial \mu \end{bmatrix}, \qquad i = 1, 2, \ldots n.
\tag{12.6}
$$

For code checking, it is useful to have the following expressions for a regular pyramid of flat rectangular $a \times b$ base, planar apex faces, apex axis normal to base, and height h:

$$
\mathbf{J} = \begin{bmatrix} \frac{1}{4}a(1-\mu) & 0 & 0 \\ 0 & \frac{1}{4}b(1-\mu) & 0 \\ -\frac{1}{4}a\xi & -\frac{1}{4}b\eta & \frac{1}{2}h \end{bmatrix}, \qquad J = \det \mathbf{J} = \frac{1}{32}abh(1-\mu)^2.
\tag{12.7}
$$

Note that at the apex $\mu = 1$, $J = 0$. Thus displacement gradients and strains are undefined at the apex.

The 6×3 strain displacement submatrix $\mathbf{B}_i$ associated with the contribution of node i is configured as

$$
\mathbf{B}_i = \begin{bmatrix} N_{xi} & 0 & 0 \\ 0 & N_{yi} & 0 \\ 0 & 0 & N_{zi} \\ N_{yi} & N_{xi} & 0 \\ 0 & N_{zi} & N_{yi} \\ N_{zi} & 0 & N_{xi} \end{bmatrix}, \qquad i = 1, 2, \ldots n.
\tag{12.8}
$$

Stacking the n submatrices $\mathbf{B}_i$ row-wise one gets the complete $6 \times 3n$ strain-displacement matrix $\mathbf{B}$ that relate strains to element node displacements:

$$
\mathbf{e} = \begin{bmatrix} e_{xx} \\ e_{yy} \\ e_{zz} \\ \gamma_{xy} \\ \gamma_{yz} \\ \gamma_{zx} \end{bmatrix} = [\mathbf{B}_1 \quad \mathbf{B}_2 \quad \ldots \quad \mathbf{B}_n] \begin{bmatrix} u_{x1} \\ u_{y1} \\ u_{z1} \\ \vdots \\ u_{zn} \end{bmatrix} = \mathbf{B}\,\mathbf{u}^{(e)}.
\tag{12.9}
$$

The stresses are linked to the strains by the elastic constitutive equation

$$
\begin{bmatrix} \sigma_{xx} \\ \sigma_{yy} \\ \sigma_{zz} \\ \tau_{xy} \\ \tau_{yz} \\ \tau_{zx} \end{bmatrix} = \begin{bmatrix} E_{11} & E_{12} & E_{13} & E_{14} & E_{15} & E_{16} \\ & E_{22} & E_{23} & E_{24} & E_{25} & E_{26} \\ & & E_{33} & E_{34} & E_{35} & E_{36} \\ & & & E_{44} & E_{45} & E_{46} \\ & & & & E_{55} & E_{56} \\ \text{symm} & & & & & E_{66} \end{bmatrix} \begin{bmatrix} e_{xx} \\ e_{yy} \\ e_{zz} \\ \gamma_{xy} \\ \gamma_{yz} \\ \gamma_{zx} \end{bmatrix},
\tag{12.10}
$$

or

$$\sigma = \mathbf{E}\mathbf{e}. \tag{12.11}$$

The stiffness and (consistent) mass matrix of the element are given by the integrals over the element volume $V^{(e)}$:

$$\mathbf{K}^{(e)} = \int_{V^{(e)}} \mathbf{B}^T \mathbf{E} \mathbf{B} \, dV = \int_{-1}^{1}\int_{-1}^{1}\int_{-1}^{1} \mathbf{B}^T \mathbf{E} \mathbf{B} \, J \, d\xi \, d\eta \, d\mu,$$

$$\mathbf{M}^{(e)} = \int_{V^{(e)}} \rho \mathbf{N}^T \mathbf{N} \, dV = \int_{-1}^{1}\int_{-1}^{1}\int_{-1}^{1} \rho \, \mathbf{N}^T \mathbf{N} \, J \, d\xi \, d\eta \, d\mu, \tag{12.12}$$

in which ρ is the mass density. These matrices are evaluated by numerical quadrature at N_p Gauss points. Assuming $\mathbf{E}$ and ρ tobe constant over the element, the numerically integrated stiffness and mass are given by

$$\mathbf{K}^{(e)} = \sum_{p=1}^{N_p} w_p \, J_p \, \mathbf{B}_p^T \mathbf{E} \, \mathbf{B}_p, \qquad \mathbf{M}^{(e)} = \sum_{p=1}^{N_p} w_p \, J_p \, \rho \, \mathbf{N}_p^T \mathbf{N}_p. \tag{12.13}$$

where $\mathbf{N}_p$, $\mathbf{B}_p$ and J_p are evaluations of $\mathbf{N}$, $\mathbf{B}$ and $J = \det \mathbf{J}$, respectively, at Gauss points defined by abscissae $\{\xi_p, \eta_p, \mu_p\}$, and the w_p are quadrature weights.

§12.4. Shape Functions of 5-Node Pyramid

To derive the shape functions of the `Pyra5` shown in Figure 12.4(b) we start with the isoparametric eight node brick. Denoting by $\{\xi_i, \eta_i, \mu_i\}$ the natural coordinates of the ith node, the brick shape functions are

$$\tilde{N}_i = \tfrac{1}{8}(1 + \xi\xi_i)(1 + \eta\eta_i)(1 + \mu\mu_i), \quad i = 1, \ldots, 8 \tag{12.14}$$

Nodes 5-6-7-8 are collapsed to apex 5, as illustrated in Figure 12.4. The shape functions of the 5-node pyramid are

$$N_i = \tilde{N}_i, \quad i = 1, 2, 3, 4,$$

$$N_5 = \tilde{N}_5 + \tilde{N}_6 + \tilde{N}_7 + \tilde{N}_8 = \tfrac{1}{2}(1 + \mu). \tag{12.15}$$

It is easily checked that these functions satisfy compatibility across the base and apex faces when the pyramid is connected to tetrahedra elements (across apex faces) and brick elements (across the base). The sum of the shape functions (12.15) is identically one. Consequently the element is conforming and complete.

The partial derivatives with respect to $\{\xi, \eta, \mu\}$ are

$$\frac{\partial N_i}{\partial \xi} = \{-\tfrac{1}{8}(1 - \eta)(1 - \mu), \quad \tfrac{1}{8}(1 - \eta)(1 - \mu), \quad \tfrac{1}{8}(1 + \eta)(1 - \mu), \quad -\tfrac{1}{8}(1 + \eta)(1 - \mu), \quad 0\}.$$

$$\frac{\partial N_i}{\partial \eta} = \{-\tfrac{1}{8}(1 - \xi)(1 - \mu), \quad -\tfrac{1}{8}(1 + \xi)(1 - \mu), \quad \tfrac{1}{8}(1 + \xi)(1 - \mu), \quad \tfrac{1}{8}(1 - \xi)(1 - \mu), \quad 0\}.$$

$$\frac{\partial N_i}{\partial \mu} = \{-\tfrac{1}{8}(1 - \xi)(1 - \eta), \quad -\tfrac{1}{8}(1 + \xi)(1 - \eta), \quad -\tfrac{1}{8}(1 + \xi)(1 + \eta), \quad -\tfrac{1}{8}(1 - \xi)(1 + \eta), \quad 1/2\}. \tag{12.16}$$

The remaining computations follow as described in the previous section. It is recommended to evaluate this element by a 5-point rule specialized to the pyramid geometry, which is described in §7.1.
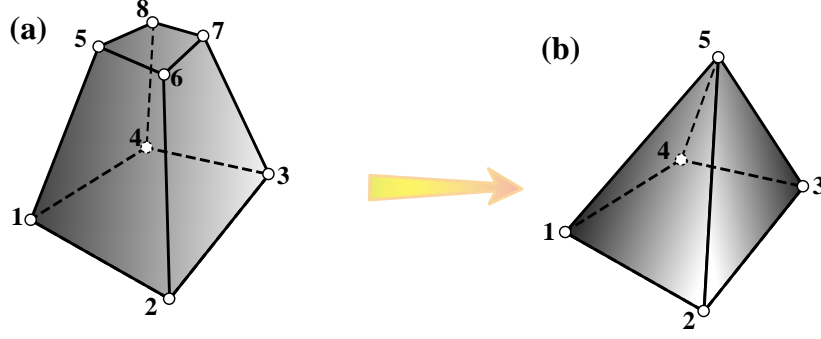
FIGURE 12.4. Morphing of 8-node brick to 5-node pyramid.

§12.5. The 13-Node Pyramid
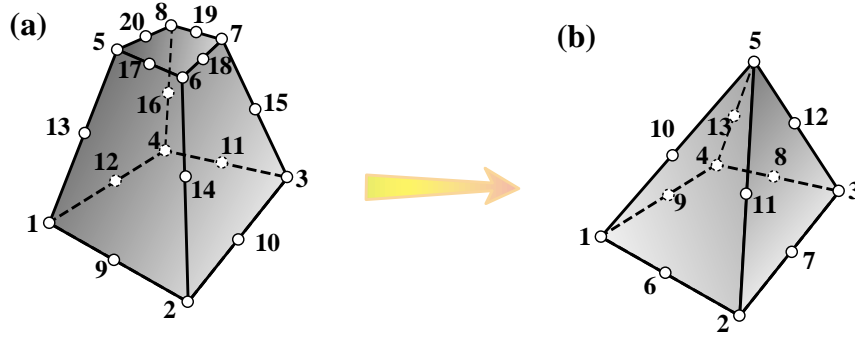
§12.5.1. Shape Functions

FIGURE 12.5. Morphing of 20-node brick to 13-node pyramid.

The shape functions of the 13-node pyramid shown in Figure 12.5(b) are derived in a two-stage process. In the first stage we start with the 20-node brick shown in Figure AFEM:Ch12:fig:TwentyNodeBrickMorphingToPyramid(a). The well known shape functions of this element are:

$$\tilde{N}_1 = -\tfrac{1}{8}(1-\xi)(1-\eta)(1-\mu)(2+\xi+\eta+\mu), \quad \tilde{N}_2 = -\tfrac{1}{8}(1+\xi)(1-\eta)(1-\mu)(2-\xi+\eta+\mu),$$
$$\tilde{N}_3 = -\tfrac{1}{8}(1+\xi)(1+\eta)(1-\mu)(2-\xi-\eta+\mu), \quad \tilde{N}_4 = -\tfrac{1}{8}(1-\xi)(1+\eta)(1-\mu)(2+\xi-\eta+\mu),$$
$$\tilde{N}_5 = -\tfrac{1}{8}(1-\xi)(1-\eta)(1+\mu)(2+\xi+\eta-\mu), \quad \tilde{N}_6 = -\tfrac{1}{8}(1+\xi)(1-\eta)(1+\mu)(2-\xi+\eta-\mu),$$
$$\tilde{N}_7 = -\tfrac{1}{8}(1+\xi)(1+\eta)(1+\mu)(2-\xi-\eta-\mu), \quad \tilde{N}_8 = -\tfrac{1}{8}(1-\xi)(1+\eta)(1+\mu)(2+\xi-\eta-\mu),$$
$$\tilde{N}_9 = \tfrac{1}{4}(1-\xi^2)(1-\eta)(1-\mu), \quad \tilde{N}_{10} = \tfrac{1}{4}(1+\xi)(1-\eta^2)(1-\mu),$$
$$\tilde{N}_{11} = \tfrac{1}{4}(1-\xi^2)(1+\eta)(1-\mu), \quad \tilde{N}_{12} = \tfrac{1}{4}(1-\xi)(1-\eta^2)(1-\mu),$$
$$\tilde{N}_{13} = \tfrac{1}{4}(1-\xi)(1-\eta)(1-\mu^2), \quad \tilde{N}_{14} = \tfrac{1}{4}(1+\xi)(1-\eta)(1-\mu^2),$$
$$\tilde{N}_{15} = \tfrac{1}{4}(1+\xi)(1+\eta)(1-\mu^2), \quad \tilde{N}_{16} = \tfrac{1}{4}(1-\xi)(1+\eta)(1-\mu^2),$$
$$\tilde{N}_{17} = \tfrac{1}{4}(1-\xi^2)(1-\eta)(1+\mu), \quad \tilde{N}_{18} = \tfrac{1}{4}(1+\xi)(1-\eta^2)(1+\mu),$$
$$\tilde{N}_{19} = \tfrac{1}{4}(1-\xi^2)(1+\eta)(1+\mu), \quad \tilde{N}_{20} = \tfrac{1}{4}(1-\xi)(1-\eta^2)(1+\mu).$$

$$(12.17)$$

Eight nodes of the brick face 5-6-7-8-17-18-19-20 are collapsed to node 5 at the pyramid apex. The resulting shape functions are

$$
\begin{aligned}
N_i^* &= \tilde{N}_i, \quad i = 1, 2, 3, 4, \\
N_i^* &= \tilde{N}_{i+3}, \quad i = 6, 7, 8, 9, \\
N_i &= \tilde{N}_{i+3}, \quad i = 10, 11, 12, 13, \\
N_5 &= \tilde{N}_5 + \tilde{N}_6 + \tilde{N}_7 + \tilde{N}_8 + \tilde{N}_{17} + \tilde{N}_{18} + \tilde{N}_{19} + \tilde{N}_{20} = \tfrac{1}{2}\mu(1 + \mu).
\end{aligned}
\tag{12.18}
$$

Note that shape functions except N_5, N_{10}, N_{11}, N_{12} and N_{13} are marked with a star (*) in (12.18) because they will be corrected in the next stage. We check displacement compatibility over the apex faces 125, 235, 345 and 415, with the shape functions of an attached 10-node tetrahedron. Compatibility is found to be violated except on the edges. To remedy this problem we inject the following "face bubble functions"

$$
\begin{aligned}
N_{125} &= \tfrac{1}{16}(1 - \xi^2)(1 - \mu^2)(1 - \eta), \quad N_{345} = \tfrac{1}{16}(1 - \xi^2)(1 - \mu^2)(1 + \eta) \\
N_{235} &= \tfrac{1}{16}(1 - \eta^2)(1 - \mu^2)(1 + \xi), \quad N_{415} = \tfrac{1}{16}(1 - \eta^2)(1 - \mu^2)(1 - \xi).
\end{aligned}
\tag{12.19}
$$

Function N_{125} only "bubbles out" over apex face 1-2-5 ($\eta = -1$); likewise N_{235}, N_{345} and N_{415} bubble out over faces 2-3-5 ($\xi = 1$), 3-4-5 ($\eta = 1$) and 4-1-5 ($\xi = -1$), respectively. They vanish over the base 1-2-3-4 ($\mu = -1$) and thus do not impair conformity with a 20-brick element attached there.

The corrections necessary to establish conformity, found through *Mathematica*, are: $N_1 = N_1^* + N_{125} + N_{415}$, $N_2 = N_2^* + N_{235} + N_{125}$, $N_3 = N_3^* + N_{345} + N_{235}$, $N_4 = N_4^* + N_{415} + N_{345}$, $N_6 = N_6^* - 2N_{125}$, $N_7 = N_7^* - 2N_{235}$, $N_8 = N_8^* - 2N_{345}$, $N_9 = N_9^* - 2N_{415}$. Adding up it is obvious that $N_1 + N_2 + N_3 + N_4 + N_6 + N_7 + N_8 + N_9 = N_1^* + N_2^* + N_3^* + N_4^* + N_6^* + N_7^* + N_8^* + N_9^*$. Thus the sum of all shape functions remain unity, and completeness is preserved. The final set of shape functions is

$$
\begin{aligned}
N_1 &= -\tfrac{1}{16}(1 - \xi)(1 - \eta)(1 - \mu)(4 + 3\xi + 3\eta + 2\xi\eta + 2\mu + \xi\mu + \eta\mu + 2\xi\eta\mu), \\
N_2 &= -\tfrac{1}{16}(1 + \xi)(1 - \eta)(1 - \mu)(4 - 3\xi + 3\eta - 2\xi\eta + 2\mu - \xi\mu + \eta\mu - 2\xi\eta\mu), \\
N_3 &= -\tfrac{1}{16}(1 + \xi)(1 + \eta)(1 - \mu)(4 - 3\xi - 3\eta + 2\xi\eta + 2\mu - \xi\mu - \eta\mu + 2\xi\eta\mu), \\
N_4 &= -\tfrac{1}{16}(1 - \xi)(1 + \eta)(1 - \mu)(4 + 3\xi - 3\eta - 2\xi\eta + 2\mu + \xi\mu - \eta\mu - 2\xi\eta\mu), \\
N_5 &= \tfrac{1}{2}\mu(1 + \mu), \\
N_6 &= \tfrac{1}{8}(1 - \xi^2)(1 - \eta)(1 - \mu)(2 + \eta + \eta\mu), \quad N_7 = \tfrac{1}{8}(1 + \xi)(1 - \eta^2)(1 - \mu)(2 - \xi - \xi\mu), \\
N_8 &= \tfrac{1}{8}(1 - \xi^2)(1 + \eta)(1 - \mu)(2 - \eta - \eta\mu), \quad N_9 = \tfrac{1}{8}(1 - \xi)(1 - \eta^2)(1 - \mu)(2 + \xi + \xi\mu), \\
N_{10} &= \tfrac{1}{4}(1 - \xi)(1 - \eta)(1 - \mu^2), \quad N_{11} = \tfrac{1}{4}(1 + \xi)(1 - \eta)(1 - \mu^2), \\
N_{12} &= \tfrac{1}{4}(1 + \xi)(1 + \eta)(1 - \mu^2), \quad N_{13} = \tfrac{1}{4}(1 - \xi)(1 + \eta)(1 - \mu^2).
\end{aligned}
\tag{12.20}
$$

§12.5.2. Compatibility Verification

The compatibility check with a quadratic tetrahedron over an apex face will be illustrated here for face 1-2-3 with midpoints 6-10-11. Evaluate (12.20) at $\eta = -1$, which is the equation of face 1-2-3. The nonzero shape functions are:

$$
\begin{aligned}
N_1 &= -\tfrac{1}{8}(1-\mu)(1-\xi)(1+\mu+\xi-\mu\xi), & N_2 &= -\tfrac{1}{8}(1-\mu)(1+\xi)(1+\mu-\xi+\mu\xi), \\
N_5 &= \tfrac{1}{2}\mu(1+\mu), & N_6 &= \tfrac{1}{4}(1-\mu)^2(1-\xi^2), \\
N_{10} &= \tfrac{1}{2}(1-\mu^2)(1-\xi), & N_{11} &= \tfrac{1}{2}(1-\mu^2)(1+\xi).
\end{aligned}
\tag{12.21}
$$

That face is taken to match that of a 10-node tetrahedron, with local corner numbers 1,2,3 and local midpoints 5-6-7 (corner 4 of the tetrahedron is away from that face). The natural coordinates of the tetrahedron are ζ_i, $i = 1, 2, 3, 4$. The equation of face 1-2-3 is $\zeta_4 = 0$. Evaluating the shape functions at $\zeta_4 = 0$ one gets

$$
\begin{aligned}
N_1 &= \zeta_1(2\zeta_1 - 1), & N_2 &= \zeta_2(2\zeta_2 - 1), \\
N_3 &= \zeta_3(2\zeta_3 - 1), & N_5 &= 4\zeta_1\zeta_2, \\
N_6 &= 4\zeta_2\zeta_3, & N_7 &= 4\zeta_1\zeta_3.
\end{aligned}
\tag{12.22}
$$

The relation between natural coordinates of the pyramid and tetrahedron over that face is $\zeta_1 = \tfrac{1}{4}(1-\xi)(1-\mu)$, $\zeta_2 = \tfrac{1}{4}(1+\xi)(1-\mu)$, and $\zeta_3 = 1 - \zeta_1 - \zeta = \tfrac{1}{2}(1+\mu)$. Substituting these relations into (12.22) the shape functions become identical to those in (12.21). This proves conformity for an arbitrary face geometry.

Compatibility verification with a 20-node brick over the pyramid base is immediate since the shape functions of the pyramid are identical over that face, and the 4 face bubbles vanish over it.

§12.5.3. Natural Derivatives

The natural derivatives are

$$
\begin{aligned}
\partial N_1/\partial\xi &= \tfrac{1}{16}(1-\eta)(1-\mu)(1+6\xi+\eta+4\xi\eta+\mu+2\xi\mu-\eta\mu+4\xi\eta\mu), \\
\partial N_2/\partial\xi &= -\tfrac{1}{16}(1-\eta)(1-\mu)(1-6\xi+\eta-4\xi\eta+\mu-2\xi\mu-\eta\mu-4\xi\eta\mu), \\
\partial N_3/\partial\xi &= -\tfrac{1}{16}(1+\eta)(1-\mu)(1-6\xi-\eta+4\xi\eta+\mu-2\xi\mu+\eta\mu+4\xi\eta\mu), \\
\partial N_4/\partial\xi &= \tfrac{1}{16}(1+\eta)(1-\mu)(1+6\xi-\eta-4\xi\eta+\mu+2\xi\mu+\eta\mu-4\xi\eta\mu), \\
\partial N_5/\partial\xi &= 0, \\
\partial N_6/\partial\xi &= -\tfrac{1}{4}\xi(1-\eta)(1-\mu)(2+\eta+\eta\mu), \quad \partial N_7/\partial\xi = \tfrac{1}{8}(1-\eta^2)(1-\mu)(1-2\xi-\mu-2\xi\mu), \\
\partial N_8/\partial\xi &= -\tfrac{1}{4}\xi(1+\eta)(1-\mu)(2-\eta-\eta\mu), \quad \partial N_9/\partial\xi = -\tfrac{1}{8}(1-\eta^2)(1-\mu)(1+2\xi-\mu+2\xi\mu), \\
\partial N_{10}/\partial\xi &= -\tfrac{1}{4}(1-\eta)(1-\mu^2), \quad \partial N_{11}/\partial\xi = \tfrac{1}{4}(1-\eta)(1-\mu^2), \\
\partial N_{12}/\partial\xi &= \tfrac{1}{4}(1+\eta)(1-\mu^2), \quad \partial N_{13}/\partial\xi = -\tfrac{1}{4}(1+\eta)(1-\mu^2),
\end{aligned}
\tag{12.23}
$$

$$\partial N_1/\partial\eta = \tfrac{1}{16}(1-\xi)(1-\mu)(1+\xi+6\eta+4\xi\eta+\mu-\xi\mu+2\eta\mu+4\xi\eta\mu),$$

$$\partial N_2/\partial\eta = \tfrac{1}{16}(1+\xi)(1-\mu)(1-\xi+6\eta-4\xi\eta+\mu+\xi\mu+2\eta\mu-4\xi\eta\mu),$$

$$\partial N_3/\partial\eta = -\tfrac{1}{16}(1+\xi)(1-\mu)(1-\xi-6\eta+4\xi\eta+\mu+\xi\mu-2\eta\mu+4\xi\eta\mu),$$

$$\partial N_4/\partial\eta = -\tfrac{1}{16}(1-\xi)(1-\mu)(1+\xi-6\eta-4\xi\eta+\mu-\xi\mu-2\eta\mu-4\xi\eta\mu),$$

$$\partial N_5/\partial\eta = 0,$$

$$\partial N_6/\partial\eta = -\tfrac{1}{8}(1-\xi^2)(1-\mu)(1+2\eta-\mu+2\eta\mu),\quad \partial N_7/\partial\eta = -\tfrac{1}{4}(1+\xi)\eta(1-\mu)(2-\xi-\xi\mu),$$

$$\partial N_8/\partial\eta = \tfrac{1}{8}(1-\xi^2)(1-\mu)(1-2\eta-\mu-2\eta\mu),\quad \partial N_9/\partial\eta = -\tfrac{1}{4}(1-\xi)\eta(1-\mu)(2+\xi+\xi\mu),$$

$$\partial N_{10}/\partial\eta = -\tfrac{1}{4}(1-\xi)(1-\mu^2),\quad \partial N_{11}/\partial\eta = -\tfrac{1}{4}(1+\xi)(1-\mu^2),$$

$$\partial N_{12}/\partial\eta = \tfrac{1}{4}(1+\xi)(1-\mu^2),\quad \partial N_{13}/\partial\eta = \tfrac{1}{4}(1-\xi)(1-\mu^2),$$

$$(12.24)$$

$$\partial N_1/\partial\mu = \tfrac{1}{8}(1-\xi)(1-\eta)(1+\xi+\eta+2\mu+\xi\mu+\eta\mu+2\xi\eta\mu),$$

$$\partial N_2/\partial\mu = \tfrac{1}{8}(1+\xi)(1-\eta)(1-\xi+\eta+2\mu-\xi\mu+\eta\mu-2\xi\eta\mu),$$

$$\partial N_3/\partial\mu = \tfrac{1}{8}(1+\xi)(1+\eta)(1-\xi-\eta+2\mu-\xi\mu-\eta\mu+2\xi\eta\mu),$$

$$\partial N_4/\partial\mu = \tfrac{1}{8}(1-\xi)(1+\eta)(1+\xi-\eta+2\mu+\xi\mu-\eta\mu-2\xi\eta\mu),$$

$$\partial N_5/\partial\mu = 1/2+\mu,\tag{12.25}$$

$$\partial N_6/\partial\mu = -\tfrac{1}{4}(1-\xi^2)(1-\eta)(1+\eta\mu),\quad \partial N_7/\partial\mu = -\tfrac{1}{4}(1+\xi)(1-\eta^2)(1-\xi\mu),$$

$$\partial N_8/\partial\mu = -\tfrac{1}{4}(1-\xi^2)(1+\eta)(1-\eta\mu),\quad \partial N_9/\partial\mu = -\tfrac{1}{4}(1-\xi)(1-\eta^2)(1+\xi\mu),$$

$$\partial N_{10}/\partial\mu = -\tfrac{1}{2}(1-\xi)(1-\eta)\mu,\quad \partial N_{11}/\partial\mu = -\tfrac{1}{2}(1+\xi)(1-\eta)\mu,$$

$$\partial N_{12}/\partial\mu = -\tfrac{1}{2}(1+\xi)(1+\eta)\mu,\quad \partial N_{13}/\partial\mu = -\tfrac{1}{2}(1-\xi)(1+\eta)\mu.$$

§12.6. The 14-Node Pyramid

§12.6.1. Shape Functions

The shape functions of the 14-node pyramid shown in Figure 12.6(a) are constructed by starting from the shape functions of the 13-node pyramid. A hierarchical shape shape function for node 14, located at the center of the base and with coordinates $\xi = \eta = 0$, $\mu = -1$, is

$$N_c = \tfrac{1}{2}(1-\xi^2)(1-\eta^2)(1-\mu),\tag{12.26}$$

This function vanishes at all nodes of the 13-node pyramid, is zero on all four apex faces, and takes the value one at the new node 14. The shape functions of nodes 1 through 4 and 6 through 9 have to be corrected by a multiple of (12.26) so they vanish at node 14 ($\xi = \eta = 0$, $\mu = -1$). The

complete shape function set is

$$
\begin{aligned}
N_1 &= -\tfrac{1}{16}(1-\xi)(1-\eta)(1-\mu)(4+3\xi+3\eta+2\xi\eta+2\mu+\xi\mu+\eta\mu+2\xi\eta\mu)+\tfrac{1}{4}N_c, \\
N_2 &= -\tfrac{1}{16}(1+\xi)(1-\eta)(1-\mu)(4-3\xi+3\eta-2\xi\eta+2\mu-\xi\mu+\eta\mu-2\xi\eta\mu)+\tfrac{1}{4}N_c, \\
N_3 &= -\tfrac{1}{16}(1+\xi)(1+\eta)(1-\mu)(4-3\xi-3\eta+2\xi\eta+2\mu-\xi\mu-\eta\mu+2\xi\eta\mu)+\tfrac{1}{4}N_c, \\
N_4 &= -\tfrac{1}{16}(1-\xi)(1+\eta)(1-\mu)(4+3\xi-3\eta-2\xi\eta+2\mu+\xi\mu-\eta\mu-2\xi\eta\mu)+\tfrac{1}{4}N_c, \\
N_5 &= \tfrac{1}{2}\mu(1+\mu), \\
N_6 &= \tfrac{1}{8}(1-\xi^2)(1-\eta)(1-\mu)(2+\eta+\eta\mu)-\tfrac{1}{2}N_c, \\
N_7 &= \tfrac{1}{8}(1+\xi)(1-\eta^2)(1-\mu)(2-\xi-\xi\mu)-\tfrac{1}{2}N_c, \\
N_8 &= \tfrac{1}{8}(1-\xi^2)(1+\eta)(1-\mu)(2-\eta-\eta\mu)-\tfrac{1}{2}N_c, \\
N_9 &= \tfrac{1}{8}(1-\xi)(1-\eta^2)(1-\mu)(2+\xi+\xi\mu)-\tfrac{1}{2}N_c, \\
N_{10} &= \tfrac{1}{4}(1-\xi)(1-\eta)(1-\mu^2), \qquad N_{11} = \tfrac{1}{4}(1+\xi)(1-\eta)(1-\mu^2), \\
N_{12} &= \tfrac{1}{4}(1+\xi)(1+\eta)(1-\mu^2), \qquad N_{13} = \tfrac{1}{4}(1-\xi)(1+\eta)(1-\mu^2), \\
N_{14} &= N_c.
\end{aligned}
$$

$$(12.27)$$

Because N_c vanishes on all apex faces, it is not necessary to recheck for compatibility with the 10-node tetrahedron.

§12.6.2. Natural Derivatives

The natural derivatives are obtained by adding the $\{\xi, \eta, \mu\}$ derivatives of N_c to the natural derivatives of Pyra13 given by (12.23) through (12.25). Defining for convenience

$$
N_{c\xi} = \frac{\partial N_c}{\partial \xi} = -\xi(1-\eta^2)(1-\mu), \; N_{c\eta} = \frac{\partial N_c}{\partial \eta} = -\eta(1-\xi^2)(1-\mu), \; N_{c\mu} = \frac{\partial N_c}{\partial \mu} = -\tfrac{1}{2}(1-\xi^2)(1-\eta^2),
$$

$$(12.28)$$

we get

$$
\begin{aligned}
\partial N_1/\partial \xi &= \tfrac{1}{16}(1-\eta)(1-\mu)(1+6\xi+\eta+4\xi\eta+\mu+2\xi\mu-\eta\mu+4\xi\eta\mu)+\tfrac{1}{4}N_{c\xi}, \\
\partial N_2/\partial \xi &= -\tfrac{1}{16}(1-\eta)(1-\mu)(1-6\xi+\eta-4\xi\eta+\mu-2\xi\mu-\eta\mu-4\xi\eta\mu)+\tfrac{1}{4}N_{c\xi}, \\
\partial N_3/\partial \xi &= -\tfrac{1}{16}(1+\eta)(1-\mu)(1-6\xi-\eta+4\xi\eta+\mu-2\xi\mu+\eta\mu+4\xi\eta\mu)+\tfrac{1}{4}N_{c\xi}, \\
\partial N_4/\partial \xi &= \tfrac{1}{16}(1+\eta)(1-\mu)(1+6\xi-\eta-4\xi\eta+\mu+2\xi\mu+\eta\mu-4\xi\eta\mu)+\tfrac{1}{4}N_{c\xi}, \quad \partial N_5/\partial \xi = 0, \\
\partial N_6/\partial \xi &= -\tfrac{1}{4}\xi(1-\eta)(1-\mu)(2+\eta+\eta\mu)-\tfrac{1}{2}N_{c\xi}, \; \partial N_7/\partial \xi = \tfrac{1}{8}(1-\eta^2)(1-\mu)(1-2\xi-\mu-2\xi\mu)-\tfrac{1}{2}N_{c\xi}, \\
\partial N_8/\partial \xi &= -\tfrac{1}{4}\xi(1+\eta)(1-\mu)(2-\eta-\eta\mu)-\tfrac{1}{2}N_{c\xi}, \; \partial N_9/\partial \xi = -\tfrac{1}{8}(1-\eta^2)(1-\mu)(1+2\xi-\mu+2\xi\mu)-\tfrac{1}{2}N_{c\xi}, \\
\partial N_{10}/\partial \xi &= -\tfrac{1}{4}(1-\eta)(1-\mu^2), \quad \partial N_{11}/\partial \xi = \tfrac{1}{4}(1-\eta)(1-\mu^2), \\
\partial N_{12}/\partial \xi &= \tfrac{1}{4}(1+\eta)(1-\mu^2), \quad \partial N_{13}/\partial \xi = -\tfrac{1}{4}(1+\eta)(1-\mu^2), \quad \partial N_{14}/\partial \xi = N_{c\xi}.
\end{aligned}
$$

$$(12.29)$$

$\partial N_1/\partial\eta = \frac{1}{16}(1-\xi)(1-\mu)(1+\xi+6\eta+4\xi\eta+\mu-\xi\mu+2\eta\mu+4\xi\eta\mu)+\frac{1}{4}N_{c\eta},$

$\partial N_2/\partial\eta = \frac{1}{16}(1+\xi)(1-\mu)(1-\xi+6\eta-4\xi\eta+\mu+\xi\mu+2\eta\mu-4\xi\eta\mu)+\frac{1}{4}N_{c\eta},$

$\partial N_3/\partial\eta = -\frac{1}{16}(1+\xi)(1-\mu)(1-\xi-6\eta+4\xi\eta+\mu+\xi\mu-2\eta\mu+4\xi\eta\mu)+\frac{1}{4}N_{c\eta},$

$\partial N_4/\partial\eta = -\frac{1}{16}(1-\xi)(1-\mu)(1+\xi-6\eta-4\xi\eta+\mu-\xi\mu-2\eta\mu-4\xi\eta\mu)+\frac{1}{4}N_{c\eta}, \quad \partial N_5/\partial\eta = 0,$

$\partial N_6/\partial\eta = -\frac{1}{8}(1-\xi^2)(1-\mu)(1+2\eta-\mu+2\eta\mu)-\frac{1}{2}N_{c\eta}, \quad \partial N_7/\partial\eta = -\frac{1}{4}(1+\xi)\eta(1-\mu)(2-\xi-\xi\mu)-\frac{1}{2}N_{c\eta},$

$\partial N_8/\partial\eta = \frac{1}{8}(1-\xi^2)(1-\mu)(1-2\eta-\mu-2\eta\mu)-\frac{1}{2}N_{c\eta}, \quad \partial N_9/\partial\eta = -\frac{1}{4}(1-\xi)\eta(1-\mu)(2+\xi+\xi\mu)-\frac{1}{2}N_{c\eta},$

$\partial N_{10}/\partial\eta = -\frac{1}{4}(1-\xi)(1-\mu^2), \quad \partial N_{11}/\partial\eta = -\frac{1}{4}(1+\xi)(1-\mu^2),$

$\partial N_{12}/\partial\eta = \frac{1}{4}(1+\xi)(1-\mu^2), \quad \partial N_{13}/\partial\eta = \frac{1}{4}(1-\xi)(1-\mu^2), \quad \partial N_{14}/\partial\eta = N_{c\eta}.$

$$(12.30)$$

$\partial N_1/\partial\mu = \frac{1}{8}(1-\xi)(1-\eta)(1+\xi+\eta+2\mu+\xi\mu+\eta\mu+2\xi\eta\mu)+\frac{1}{4}N_{c\mu},$

$\partial N_2/\partial\mu = \frac{1}{8}(1+\xi)(1-\eta)(1-\xi+\eta+2\mu-\xi\mu+\eta\mu-2\xi\eta\mu)+\frac{1}{4}N_{c\mu},$

$\partial N_3/\partial\mu = \frac{1}{8}(1+\xi)(1+\eta)(1-\xi-\eta+2\mu-\xi\mu-\eta\mu+2\xi\eta\mu)+\frac{1}{4}N_{c\mu},$

$\partial N_4/\partial\mu = \frac{1}{8}(1-\xi)(1+\eta)(1+\xi-\eta+2\mu+\xi\mu-\eta\mu-2\xi\eta\mu)+\frac{1}{4}N_{c\mu}, \quad \partial N_5/\partial\mu = 1/2+\mu,$

$\partial N_6/\partial\mu = -\frac{1}{4}(1-\xi^2)(1-\eta)(1+\eta\mu)-\frac{1}{2}N_{c\mu}, \quad \partial N_7/\partial\mu = -\frac{1}{4}(1+\xi)(1-\eta^2)(1-\xi\mu)-\frac{1}{2}N_{c\mu},$

$\partial N_8/\partial\mu = -\frac{1}{4}(1-\xi^2)(1+\eta)(1-\eta\mu)-\frac{1}{2}N_{c\mu}, \quad \partial N_9/\partial\mu = -\frac{1}{4}(1-\xi)(1-\eta^2)(1+\xi\mu)-\frac{1}{2}N_{c\mu},$

$\partial N_{10}/\partial\mu = -\frac{1}{2}(1-\xi)(1-\eta)\mu, \quad \partial N_{11}/\partial\mu = -\frac{1}{2}(1+\xi)(1-\eta)\mu,$

$\partial N_{12}/\partial\mu = -\frac{1}{2}(1+\xi)(1+\eta)\mu, \quad \partial N_{13}/\partial\mu = -\frac{1}{2}(1-\xi)(1+\eta)\mu, \quad \partial N_{14}/\partial\mu = N_{c\mu}.$

$$(12.31)$$

§12.6.3. *Local Node Mapping

The local numbering of the Pyra14 element has to be mapped as shown in Figure 12.6 for compatibility with Lagrangian solid elements of certain codes that follow an IJK scheme. This is easily done in the implementation of the shape functions by apropriate array re-indexing.
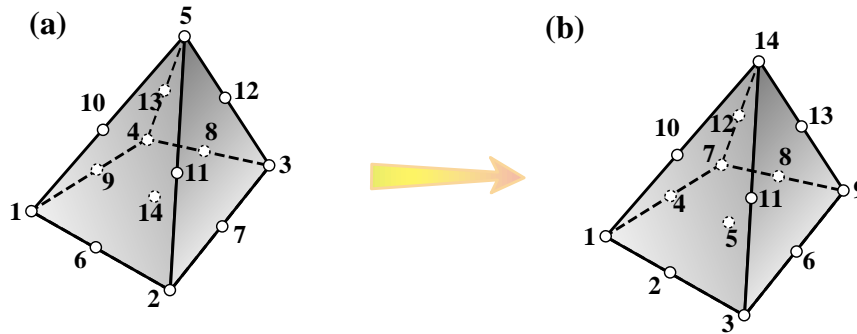

FIGURE 12.6. Mapping of local node numbering of 14-node pyramid.

§12.7. Numerical Quadrature

The minimum number of Gauss points to get a rank-sufficient stiffness for the Pyra5, Pyra13 and Pyra14 elements is 2, 6 and 6, respectively. The minimum number to get a full-rank mass matrix is 5, 13 and 14, respectively (that is, same as the number of nodes). These counts can be amply covered by the standard $2 \times 2 \times 2$ product rule for Pyra5 and the $3 \times 3 \times 3$ product rule for Pyra13

and `Pyra14`. However, it is possible to reduce the number of points by using rules customized to the pyramid geometry. New rules of this nature, developed with *Mathematica*, are presented here.

The new rules are "$\{\xi, \mu\}$ symmetric" in the following sense: if $\{\xi_i = \alpha, \eta_i = \beta, \mu_i = \gamma\}$ is a Gauss point with weight w_i, the four locations $\{\pm\alpha, \pm\beta, \gamma\}$ are Gauss points with the same weight w_i. This grouping is called a 4-point star. It is appropriate for the pyramid geometry, which treats the height direction μ differently from $\{\xi, \eta\}$. A consequence is that Gauss points appear in multiples of 4 except if $\alpha = \beta = 0$, in which case they coalesce to one point on the apex axis.

Other constraints on the new rules are the usual ones in FEM work: all points must be inside the element, and all weights must be positive.

Table 12.1. The 1-point Pyramid Gauss Rule

Point i	Abscissa $\{\xi_i, \eta_i, \mu_i\}$	Weight w_i
1	$\{0, 0, -1/2\}$	$128/27$

Exact (reference pyramid): 1, μ, and any function odd in ξ or η, e.g. $\xi, \eta, \xi\eta, \xi\mu^2 \ldots$

§12.7.1. Rules with 1 and 5 Points

The simplest rule has one point at the centroid and is defined in Table 12.1. The exactness remark in Table 12.1 applies to the "reference pyramid" which has a flat rectangular base. The rule is appropriate for computation of volumes and first moments. As such it would useful for consistent body loads and lumped mass of the low order element Pyra5.

The next useful rule has five points and is specified in Table 12.2. It is made up of a 4-point star plus one point located on the apex axis. It is recommended for the Pyra5 element in lieu of the standard $2 \times 2 \times 2$ product rule, since it gives rank-sufficient (and well conditioned) $\mathbf{K}$ and $\mathbf{M}$ with a 5:8 reduction in the number of integration points.

§12.7.2. Rules with 6 through 9 Points

Three more $\{\xi, \eta\}$ symmetric rules with 6, 8 and 9 points were constructed with the objective of using them for the stiffness matrix of `Pyra13` and `Pyra14`. These are made up with one, two and two 4-point stars, respectively, complemented with two, zero and one apex-axis points, respectively. Although tests show that they provide a rank-sufficient $\mathbf{K}$, they are not recommended for the following reason.

When the 8-node serendipity iso-P quadrilateral stiffness is underintegrated by a 2×2 product Gauss rule, it is well known that the element develops a spurious zero-energy mode (ZEM) that has zero strains at the 4 Gauss points. That ZEM has two opposite sides "bulging parabolically" outward whereas the other two sides bulge inward.

The analogous pattern for the `Pyra13` and `Pyra14` elements is a in-out bulging base mode that propagates with a similar shape in the apex direction, vanishing at the apex. Under the 6-, 8- and 9-point integration rules this pattern becomes a low energy mode (LEM), characterized by an

Table 12.2. The 5-point Pyramid Gauss Rule

Point i	Abscissa $\{\xi_i, \eta_i, \mu_i\}$	Weight w_i
1	$\{-g_1, -g_1, g_2\}$	w_1
2	$\{g_1, -g_1, g_2\}$	w_1
3	$\{g_1, g_1, g_2\}$	w_1
4	$\{-g_1, g_1, g_2\}$	w_1
5	$\{0, 0, g_3\}$	w_2

$g_1 = (8/5)\sqrt{2/15} = 0.584237394672177188,$
$g_2 = -2/3, g_3 = 2/5, w_1 = 81/100, w_2 = 125/27.$

Exact (reference pyramid): $1, \mu, \xi^2, \eta^2, \mu^2, \xi\eta, \xi\mu, \eta\mu, \xi^2\mu, \eta^2\mu,$
as well as any function odd in ξ or η, such as $\xi, \eta, \xi\eta, \xi\mu, \eta\mu \ldots$

Table 12.3. Pyra13-Pyra14 Deformational Stiffness Condition
Numbers for Various Integration Rules

Quadrature rule	Pyra13 $C^d(\mathbf{K})$	Pyra14 $C^d(\mathbf{K})$
new: 6 points	83324.5	∞
new: 8 points	7784220	6569760
standard $2 \times 2 \times 2$	∞	∞
new: 9 points	31370.7	26643.3
new: 13 points	480.14	416.808
standard $3 \times 3 \times 3$	104.01	99.995

Elements have flat square bases 2×2, height $h = 3$,
isotropic material with $\nu = 0$.

eigenvector $\mathbf{v}_{LEM}$. This is not actually a spurious mode but it has a very low associated eigenvalue $\lambda_{min} = \lambda_{LEM} = \mathbf{v}_{LEM}^T \mathbf{K} \mathbf{v}_{LEM} > 0$. Here the designation λ_{min} ignores the six rigid body modes (RBMs) which have zero associated eigenvalues. The ratio

$$C^d(\mathbf{K}) = \lambda_{max}/\lambda_{min} \quad \text{(with 6 RBMs excluded)} \tag{12.32}$$

is called the deformational stiffness condition number. Table 12.3 collects the $C^d(\mathbf{K})$ computed for the new rules as well as the standard $2 \times 2 \times 2$ and $3 \times 3 \times 3$ product rules, for an element of good aspect ratio. As expected, under the $2 \times 2 \times 2$ product rule the LEM becomes a ZEM (spurious mode) and $C^d = \infty$. Of the new pyramid-customized rules only the 13-point quadrature compares well with the more expensive $3 \times 3 \times 3$ product rule. Consequently rules with 6, 8 and 9 points are not recommended for the Pyra13 and Pyra14 elements.

Table 12.4. The 13-point Pyramid Gauss Integration Rule

Point i	Abscissa $\{\xi_i, \eta_i, \mu_i\}$	Weight w_i
1	$\{-g_1, -g_1, g_4\}$	w_1
2	$\{g_1, -g_1, g_4\}$	w_1
3	$\{g_1, g_1, g_4\}$	w_1
4	$\{-g_1, g_1, g_4\}$	w_1
5	$\{-g_2, 0, g_5\}$	w_2
6	$\{g_2, 0, g_5\}$	w_2
7	$\{0, -g_2, g_5\}$	w_2
8	$\{0, g_2, g_5\}$	w_2
9	$\{0, 0, g_6\}$	w_3
10	$\{-g_3, -g_3, g_7\}$	w_4
11	$\{g_3, -g_3, g_7\}$	w_4
12	$\{g_3, g_3, g_7\}$	w_4
13	$\{-g_3, g_3, g_7\}$	w_4

$g_1 = (7/8)\sqrt{35/59} = 0.673931986207731726,$

$g_2 = (224/37)\sqrt{336633710/33088740423} = 0.610639618865075532,$

$g_3 = (1/56)\sqrt{37043/35} = 0.580939660561084423,$

$g_4 = -1/7 = -0.1428571428571428571,$

$g_5 = -9/28 = -0.321428571428571429,$

$g_6 = 1490761/2842826 = 0.524394036075370072,$

$g_7 = -127/153 = -0.830065359477124183,$

$w_1 = 170569/331200 = 0.515003019323671498,$

$w_2 = 276710106577408/1075923777052725 = 0.2571837452420646589,$

$w_3 = 10663383340655070643544192/4310170528879365193704375$
$\quad = 2.474004977113405936,$

$w_4 = 12827693806929/30577384040000 = 0.419515737191525950.$

Exact (reference pyramid): $1, \mu, \xi^2, \eta^2, \mu^2, \xi^2\mu, \eta^2\mu, \mu^3, \xi^2\eta^2, \xi^2\mu^2,$
$\eta^2\mu^2, \xi^2\mu^3, \eta^2\mu^3, \xi^2\eta^2\mu, \xi^2\eta^2\mu^2,$ and any function odd in ξ or η.

§12.7.3. A Rule with 13 Points

The 13-point rule mentioned above is defined in Table 12.4. It is made up of three 4-point stars plus one point on the apex axis. As noted, it is recommended for the computation of the stiffness matrix of Pyra13 and Pyra14. For the mass matrix of Pyra14 it falls short of giving full rank since 14 (=42/3) points would be needed, but that deficiency is not usually important* in element assemblies.

One effect of the 13-point rule should be noted. Consistent node forces for face pressures or body loads for Pyra13 and Pyra14 are not exactly the same as those obtained if the $3 \times 3 \times 3$ rules

---

* Unless the mass matrix is inverted by itself, which rarely happens outside of explicit dynamics.
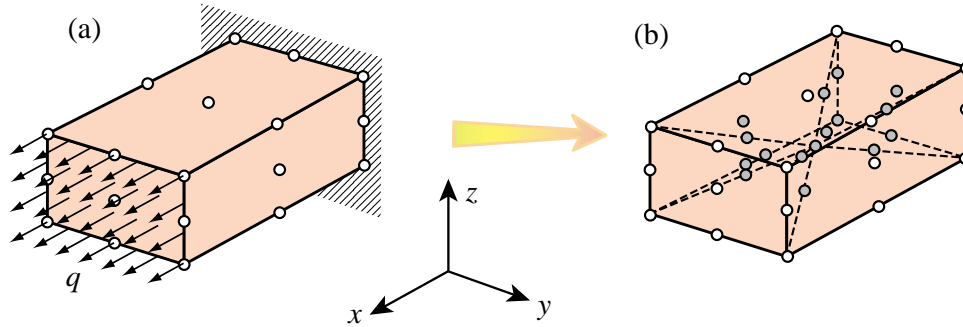
FIGURE 12.7. Patch test on cubic volume: (a) prescribed force patch test illustrated on a
`Pyra14` assembly; (b) division of volume into six `Pyra14` elements.

is used. The reason is that some terms such as $\xi^2\eta^2\mu^4$, which appear when the variation of the Jacobian over faces or the volume is considered, are not exactly integrated by the 13-point rule.

The difference is not very significant: about 1 to 5% for uniform face pressures, but the discrepancy it should be taken into account when running tests with few elements. In particular, *patch tests involving Py13 and Pyra14 should be run using the $3 \times 3 \times 3$ rule for the pyramids*. This recommendation is discussed further in the next section.

§12.8. Patch Tests

A series of patch tests were run to verify the formulation of the new `Pyra13` and `Pyra14` elements as well as their mixability with 10-node tetrahedra. The tests were carried out as follows.

1. A cube-like prismatic volume was divided into six pyramidal volumes by injecting a center node, as depicted in Figure 12.7. The pyramid bases are the volume faces and the center node is the apex of all pyramids. Figure 12.8 illustrates the volume decomposition in more detail.

2. Each pyramid volume was treated as either a single pyramid element, or as a combination of two 10-node tetrahedra (Tet10) elements, as shown in Figure 12.8 for one of the pyramids. The two-tet configuration was implemented as a pyramid macroelement for convenience in mix-and-match tests. The Tet10 elements were integrated exactly using a 4-point Gauss rule. The replacement was done randomly.

3. The cube was subjected to prescribed displacement and prescribed force patch tests for uniform stress-strain states. Figure 12.7 pictures a force patch test in which one face of the cubic volume is subject to a uniform normal surface traction q while the opposite face is fixed (but allowed to contract of expand); the result should be a uniform $\sigma_{xx} = q$ over all elements.

Tests with pyramid-only configurations were successful for the Pyra5, `Pyra13` and `Pyra14` models. Mixtures of `Tet10` elements with `Pyra13` and `Pyra14` elements initially failed the test by about 25%. This was traced back to two error sources:

(i) The face-bubble corrective shape functions (19) were missing decay-away-from-face functions. This was responsible for about 22% error, which was fixed when the proper decay functions were incorporated into the shape function sets (12.20) and (12.27).
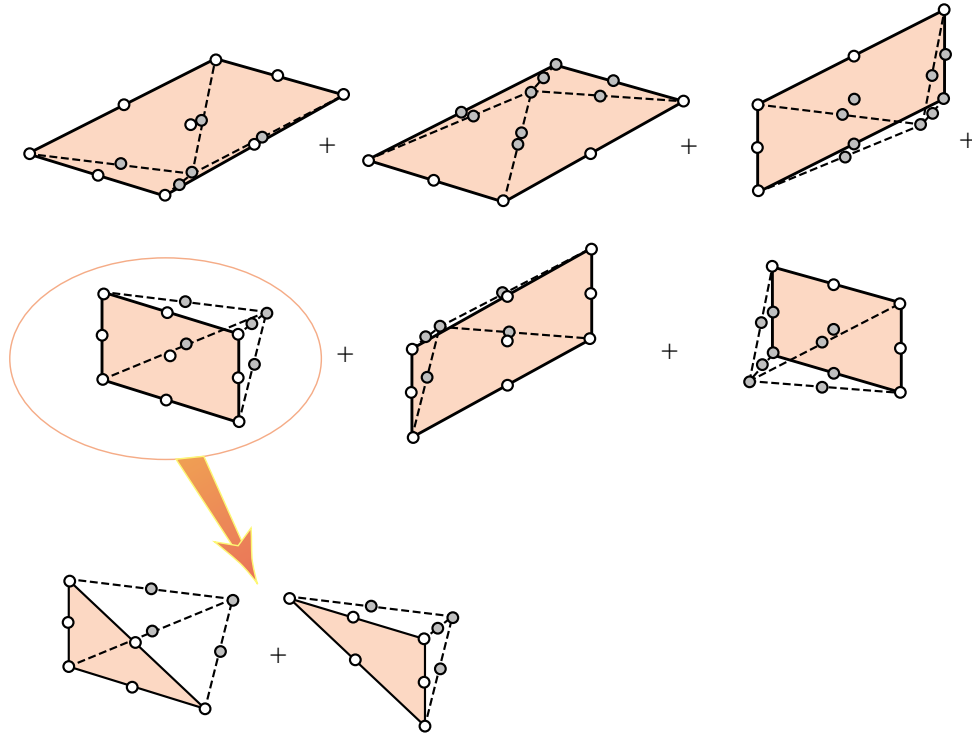
FIGURE 12.8. `Pyra14` elements resulting from the patch test decomposition of Figure 12.7(b). One of them is shown replaced by a two-`Tet10` macroelement to check `Pyra14-Tet10` mixability. These replacements were done randomly.

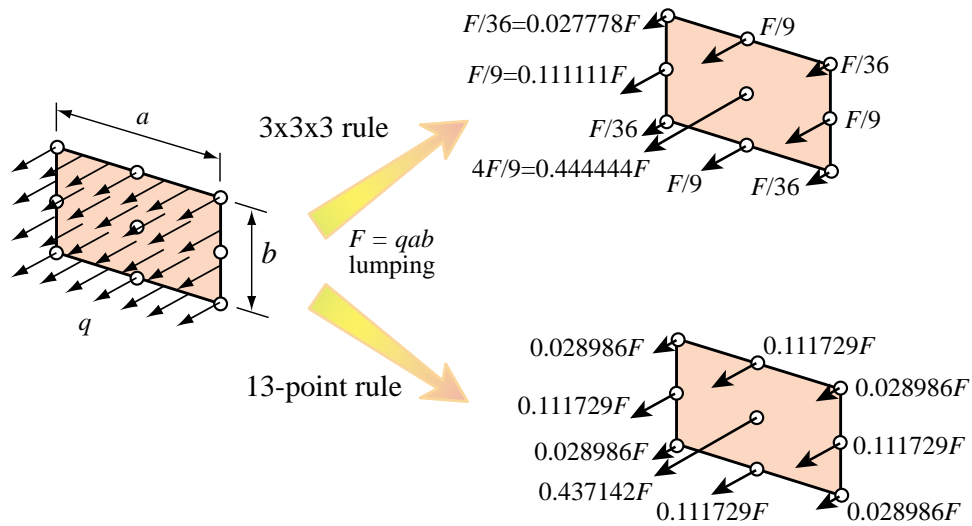
FIGURE 12.9. Consistent forces for pressure over a 9-node quadrilateral face.

(ii) The element integration rule effect discussed in §7.3 was responsible for the remaining error of about 2-3%. This was eliminated by using the $3 \times 3 \times 3$ rule and the correct consistent node forces for face pressures.

The last effect is further illustrated in Figure 12.9. This shows the consistent node forces associated

to a uniform normal surface traction q acting over a $a \times b$ 9-node rectangular face, which corresponds to a Pyra14 patch test of the type depicted in Figure 12.7(a). For the $3 \times 3 \times 3$ rule the consistent forces follows the well know proportion $16 : 4 : 1$ for center:midpoints:corners. If the 13-point rule is used, the consistent forces change by 1-5%. Similar effects were observed in Pyra13 and apex faces.